Pulse Radiolysis of 4,4′-Bipyridyl Aqueous Solutions at Elevated Temperatures: Spectral Changes and Reaction Kinetics up to 400 °C

Mingzhang Lin, Yosuke Katsumura,* Hui He, Yusa Muroya, Zhenhui Han, Toyoaki Miyazaki, and Hisaaki Kudo

Nuclear Engineering Research Laboratory, School of Engineering, The University of Tokyo, 2-22 Shirakata Shirane, Tokaimura, Nakagun, Ibaraki 319-1188, Japan

Received: November 29, 2004; In Final Form: January 25, 2005

The spectral changes as well as the reaction kinetics of the transient species of 4,4′-bipyridyl (4,4′-bpy) have been experimentally investigated by pulse radiolysis techniques up to 400 °C. The results show that the transient species such as OH adduct 4,4′-bpyOH•, monoprotonated electron adduct 4,4′-bpyH•, and doubly protonated electron adduct 4,4′-bpyH_2^{+}• have 15−20 nm blue shifts from room temperature to 400 °C. For a deaerated neutral solution of 4,4′-bpy in the presence of *tert*-butyl alcohol, ethanol, or NaCOOH, the doubly protonated electron adduct is the main transient species at room temperature. But at temperatures > 350 °C, a monoprotonated form, the N-hydro radical 4,4′-bpyH•, becomes predominant. Interestingly, at room temperature, CO_2^{-}• could not efficiently react with 4,4′-bpy, but the reaction was accelerated with increasing temperature; at 350 °C, this reaction completed within 2 μs. Using an alkaline solution (pH = 11.5) of 4,4′-bpy in the presence of *tert*-butyl alcohol, we studied the N-hydro radical 4,4′-bpyH• from room temperature to 400 °C at 25 MPa. An estimation of the temperature-dependent $G(e_{aq}^{-})$ at 25 MPa agrees with our previous result with methyl viologen as a scavenger.

1. Introduction

Supercritical water is a peculiar medium, which is very different from water in the conventional phases—gas, liquid, and solid phase. As an environmentally friendly "green" solvent, it has many applications such as the destruction of hazardous waste, the synthesis of new materials, etc.[1−4] Recently it has been proposed also to use supercritical water as a coolant for nuclear power plants, so-called supercritical water cooled reactor (SCWR).[5] Study of the water radiolysis and radiation-induced reactions is thus inevitable. For the modeling of water radiolysis in nuclear reactors, the basic data on the rate constants of a set of reactions as well as the radiolytic yields of water decomposition products are necessary. In our recent work, methyl viologen has been used as a scavenger for the estimation of radiolytic yields of water decomposition products, $G(e_{aq}^{-})$ and $\{G(e_{aq}^{-}) + G(OH) + G(H)\}$, from room temperature to 400 °C.[6] However, it has been shown that methyl viologen has a problem with thermal stability at elevated temperatures, although it is still usable for pulse radiolysis studies of supercritical water under conditions of relatively high flow rate. Its decomposition product in supercritical water has been identified to be 4,4′-bpy.[6]

Therefore, in the present work, we choose 4,4′-bpy to study. As a scavenger of water decomposition products, 4,4′-bpy has the following advantages. First, the thermal stability of 4,4′-bpy is expected to be better because it is the pyrolysis product of methyl viologen. In fact, we have been searching a suitable scavenging system for temperatures > 400 °C because the core average temperature of SCWR will be > 500 °C.[7] Second, 4,4′-bpy and methyl viologen are analogues and their reactivities are very similar.[8,9] The absorption coefficients of the transient species are fairly high. This is important for the studies in low-density supercritical water, where the apparent absorbance (without correction for density) is much lower than that at room temperature. Third, in neutral medium, 4,4′-bpy is electrically neutral. This is also a favorable factor because the solubility of salts decreases dramatically in supercritical water.[10]

As electron acceptors and electron carriers, 4,4′-bpy as well as its derivatives have been intensively studied by pulse radiolysis techniques[8,9,11,12] and by time-resolved resonance Raman spectroscopy.[13] The reactivity of 4,4′-bpy toward hydrated electron, H atom, and OH radical, as well as the pH-dependent spectral properties, have been reported.[8,9] However, to our knowledge, there is no report of the temperature effects on the pulse radiolysis of 4,4′-bpy aqueous solution.

In addition, 4,4′-bpy is the main pyrolysis product of methyl viologen (known as paraquat) which is one of the most dangerous and controversial herbicides in the world.[14] Nowadays the global ban and phaseout of the production and use of paraquat have been strongly called for.[15] For the treatment of paraquat-contaminated waters, photodegradation methods and adsorption by activated carbon have been reported.[16,17] But for complete destruction of paraquat, supercritical water oxidation could be one of the most effective and more "green" approaches since it has been proved to be very powerful for the destruction of organic compounds.[2] This study could provide useful information for the supercritical water oxidation (SCWO) of paraquat, for example, the oxidation reaction with OH radical, etc. In this work, we mainly focused on the spectral changes and reaction kinetics of the transient species in various scavenging systems from room temperature to 400 °C. In a forthcoming paper, we will report the results obtained at temperatures > 400 °C.

* Address correspondence to this author at the Nuclear Engineering Research Laboratory, School of Engineering, The University of Tokyo, Hongo 7-3-1, Bunkyo-ku, Tokyo 113, Japan; fax/telephone +81-3-5841-8624; e-mail katsu@q.t.u-tokyo.ac.jp.

10.1021/jp044590p CCC: $30.25 © 2005 American Chemical Society
Published on Web 03/03/2005

2. Experimental Section

4,4′-Bipyridyl [$C_{10}H_8N_2$], sodium formate, ethanol, and *tert*-butyl alcohol were purchased from Wako Pure Chemical Industries, Ltd., and used as received. Fresh solutions were prepared with Millipore-filtered water (resistivity > 18.2 MΩ• cm). pH was adjusted by addition of $HClO_4$ or NaOH. The solutions were immediately purged with argon or N_2O after the measurement of pH. In the case of alcohol as a scavenger, to compensate for the loss of alcohol after extensive gas purging, an appropriate amount of alcohol was added to the bulk solution every 2−3 h.

The pulse radiolysis experiments were carried out at the Nuclear Engineering Research Laboratory, University of Tokyo. The energy and pulse duration of the electron beam were 28 MeV and 2, 10, or 50 ns, respectively. The high-temperature/pressure flow cell was made of Hastelloy HC22 with sapphire windows. Details of the apparatus were described elsewhere.[18,19] Here we point out only some important parameters. The highest temperature and pressure for the flow cell guaranteed by the factory (Taiatsu Techno) are 400 °C and 40 MPa, respectively. The optical path length is 15 mm. The flow system is composed of a pump, a preheater, a heater, a back-pressure regulator, and a power supply with a temperature control unit. Four thermocouples are used to monitor temperatures at the preheater and the heater; one of these thermocouples is placed inside the solution for monitoring the temperature of irradiated samples.

For the measurement of the rate constants of the reaction between 4,4′-bpy and hydrated electron, an experimental setup with two HPLC pumps was employed so that the initial concentration of 4,4′-bpy could be adjusted by changing the flow rate of the pumps. This allows us to measure the rate constant at a given temperature under the same beam conditions.

The dosimetry was done with the 10 mM KSCN dosimeter saturated with N_2O. A value of $G\epsilon[(SCN)_2^{\bullet -}] = 5.2 \times 10^{-4}$ m^2/J at 475 nm was used.[20] The dose was normally adjusted between 10 and 90 Gy/pulse. The density of water is temperature-dependent and it was assumed that the absorbed energy is proportional to the density. We could not measure the dose pulse by pulse because of the use of full-metal high-temperature cell, but the dose fluctuation is less than 5% during a daylong experiment.

3. Results and Discussion

3.1. Thermal Stability and Pulse Radiolysis of 4,4′-Bpy at Room Temperature. Before pulse radiolysis experiments, we tested the thermal stability of an aqueous solution of 25 μM 4,4′-bpy. The solution flowed through the high-temperature/pressure cell with a flow rate of 3 mL/min (corresponds to 12 s residence time at room temperature) at different temperatures. Samples were collected at the exit of the pressure regulator and then measured at ambient temperature on a UV−vis spectrometer within the wavelength range 200−300 nm. At room temperature, an absorption peak is located at 239 nm; with increasing temperatures up to 450 °C, the peak position and the spectral shape, as well as the absorbance at 239 nm, have not shown notable change. These facts suggest that there is no pyrolysis of 4,4′-bpy within the temperature range tested. Therefore we may do pulse radiolysis experiments without the problem of decomposition of 4,4′-bpy, at least up to 450 °C. However, in the present work, the temperature is limited at 400 °C.

It is important to point out that there are various forms of 4,4′-bpy according to the acid−base properties: $bpyH_2^{2+}$ ($pK_a = -0.2$) and $bpyH^+$ ($pK_a = 4.25$).[21,22] The absorption spectra

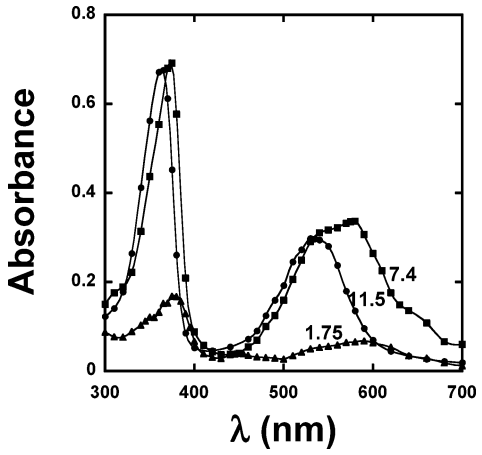

Figure 1. Pulse radiolysis of 0.5 mM 4,4′-bpy solutions in the presence of 0.2 M *tert*-butyl alcohol at different pH values with a dose of 75 Gy. For pH 7.4 and 11.5 the absorbencies were recorded at 500 ns, while for pH 1.75 they were recorded at 4 μs after the electron pulse.

of transient species as well as the reactivity are strongly dependent on pH. Figure 1 shows the transient spectra of 4,4′-bpy aqueous solutions at various pH at room temperature. For acidic solution (pH 1.75), there are at least three absorption bands, which are at 375, 450, and 580 nm. The radical forms 4,4′-$bpyH_2^{+\bullet}$ and 4,4′-$bpyH_3^{+\bullet}$ (including H adduct on ring carbons and on N-atom), as well as the dimer of 4,4′-$bpyH_2^{+\bullet}$, have been attributed to these absorption bands.[9] For neutral solution, two main absorption bands are presented, which are at 375 and 580 nm. They characterize the N,N′-dihydro radical cation 4,4′-$bpyH_2^{+\bullet}$[9,13] according to

$$H_2O \xrightarrow{\gamma,e^-} e_{aq}^-, H, OH, H_2, H_2O_2, HO_2 \quad (1)$$

$$4,4'\text{-bpy} + e_{aq}^- + H_2O \rightarrow 4,4'\text{-bpyH}^\bullet + OH^-$$

$$k = 2.2 \times 10^{10}\ M^{-1}\ s^{-1}\ (pH\ 8.3)^9 \quad (2)$$

$$4,4'\text{-bpyH}^\bullet + H^+ \rightleftharpoons 4,4'\text{-bpyH}_2^{+\bullet} \quad (3a)$$

or

$$4,4'\text{-bpyH}^\bullet\cdots HOH \rightleftharpoons 4,4'\text{-bpyH}_2^{+\bullet} + OH^- \quad (3b)$$

because in aqueous solution the unquaternized 4,4′-bpy N atom is H-bonded.

It is noted that, for reaction 2, the reaction of e_{aq}^- with 4,4′-bpy should result first in the formation of the radical anion 4,4′-$bpy^{-\bullet}$, which has an absorption spectrum similar to that of 4,4′-$bpyH_2^{+\bullet}$ ($\lambda_{max} = 385, 570$ nm).[13,23−25] However, the spectrum at pH 7.4 in Figure 1 is apparently not of the radical anion 4,4′-$bpy^{-\bullet}$ because it is strongly pH-dependent, as we can see below. The radical anion undergoes rapid protonation on nitrogen to form N-hydro radical 4,4′-bpyH• and then 4,4′-$bpyH_2^{+\bullet}$.[13,26]

In alkaline solution, there are also two absorption bands: 360 and 530 nm. The transient species was assigned to N-hydro radical 4,4′-bpyH•.[13]

In the present work, we focused mainly on the neutral solutions in the presence of various scavengers and an alkaline solution in the presence of *tert*-butyl alcohols. We did not deal with acidic solutions at elevated temperatures because the problem of the interaction of acid with the Hastelloy cell will arise.

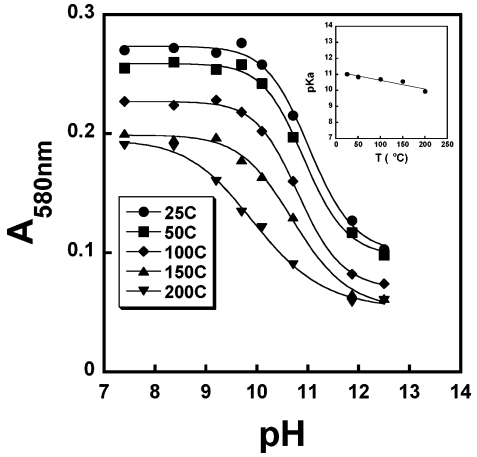

Figure 2. Absorbencies at different temperatures vary with initial pH values measured at room temperature of 0.5 mM 4,4′-bpy/0.2 M *tert*-butyl alcohol aqueous solution. Pressure was 25 MPa. Inset: pK_a as a function of temperature.

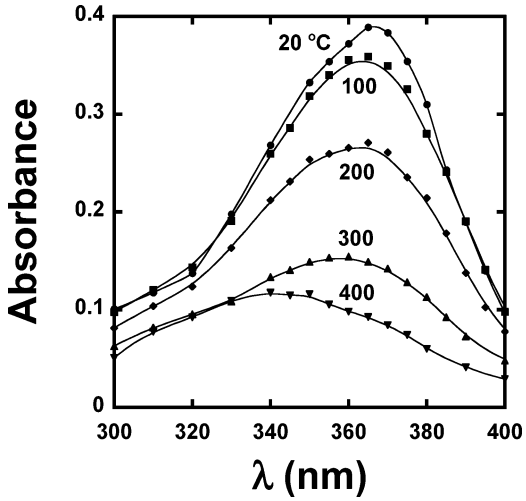

Figure 3. Temperature-dependent transient absorption spectra of OH adducts to 4,4′-bpy obtained by pulse radiolysis of 0.5 mM 4,4′-bpy in N_2O-saturated solutions.

It was found that there existed an equilibrium between doubly protonated and monoprotonated electron adducts:

$$4,4'\text{-bpyH}_2^{+\bullet} \rightleftharpoons 4,4'\text{-bpyH}^{\bullet} + \text{H}^+ \qquad (4)$$

The pK_a of this reaction was estimated to be 10.5 by Simić and Ebert.[8] To elucidate the temperature effect on this equilibrium, we prepared a series of aqueous solutions of 0.5 mM 4,4′-bpy in the presence of 0.2 M *tert*-butyl alcohol at different pH and measured the absorbance at 580 nm by pulse radiolysis at 25, 50, 100, 150, and 200 °C. From Figure 2, which plots the change of absorbance at 580 nm at various temperatures versus the room-temperature pH, we may obtain the pK_a in units of room-temperature pH of 4,4′-bpyH$_2^{+\bullet}$ varying with temperatures, as shown in the inset of Figure 2. From this figure, it is clear that the increase of temperature is favorable for 4,4′-bpyH$^{\bullet}$. This is reasonable if compared with the temperature effect of water dissociation. As is known, the ion product of water increases within the temperature range 0−300 °C (however, in supercritical water, the ion product is very small).[10] The pK_w is 14 at room temperature while it is about 11.4 at 300 °C.

3.2. OH Adducts of 4,4′-Bpy. Figure 3 was obtained by pulse radiolysis of an N_2O-saturated solution of 0.5 mM 4,4′-bpy. The hydrated electrons produced by water radiolysis are converted to $^{\bullet}$OH radicals:

$$e_{aq}^- + N_2O \rightarrow N_2 + {}^{\bullet}OH + OH^- \qquad k_5 = 9.1 \times 10^9\ M^{-1}\ s^{-1}\ (\text{ref } 27) \quad (5)$$

This leads to the formation of additional $^{\bullet}$OH radicals and creates nearly a one-radical system consisting of $^{\bullet}$OH in the aqueous solution. The $^{\bullet}$OH radicals react with 4,4′-bpy to form OH adducts [4,4′-bpyOH]$^{\bullet}$.

Unlike H-adducts and electron adducts of 4,4′-bpy (Figure 1), at room temperature, the absorption spectrum of OH adducts shows only one absorption band with $\lambda_{max} = 365$ nm, in agreement with the literature data.[8] Judging from the rather intense absorption and from the similarity with the OH adducts to nitrobenzene,[28] this absorption band is assigned to $\pi \rightarrow \pi^*$ transition absorption band. $^{\bullet}$OH radicals are expected to add to the two possible positions (ortho and meso) of the pyridyl ring,[8] but the absorption bands of the two OH adducts are undistinguishable.

As shown in Figure 3, λ_{max} shifts to shorter wavelength (a blue shift) with increasing temperature: at 400 °C, $\lambda_{max} = 350$ nm. This blue solvatochromic shift of the $\pi \rightarrow \pi^*$ absorbance of [4,4′-bpyOH]$^{\bullet}$ indicates that the excited state is more polar than the ground state. Decrease of solution density and reduced hydrogen bonding as well as reduced solvent (water) polarity with increasing temperature result in less stabilization of the excited state and a shift of λ_{max} to higher energies.[29] Similar behavior has been reported for benzophenone[30] and nitrobenzene[28] in subcritical and supercritical water.

Then we studied the reactivity of 4,4′-bpy toward $^{\bullet}$OH radical. Since the absorption band of $^{\bullet}$OH radical is in the deep UV region and its absorption coefficient is low ($\epsilon_{235nm} \approx 590$ L mol^{-1} cm^{-1}),[31] and also 4,4′-bpy has a strong absorption band in the same region, a direct observation of the decay of $^{\bullet}$OH radical is rather difficult. Therefore, we monitored the formation of [4,4′-bpyOH]$^{\bullet}$ at 360 nm rather than the decay of $^{\bullet}$OH radical. By fitting the kinetic signals, we may obtain the rate constants at different temperatures. The rate constant at 20 °C was 6.6×10^9 M^{-1} s^{-1} (pH 7.4), which is comparable to the reported data, 5.3×10^9 M^{-1} s^{-1} (pH 9.3).[8] Figure 4 shows the Arrhenius plot of the reaction between $^{\bullet}$OH and 4,4′-bpy from room

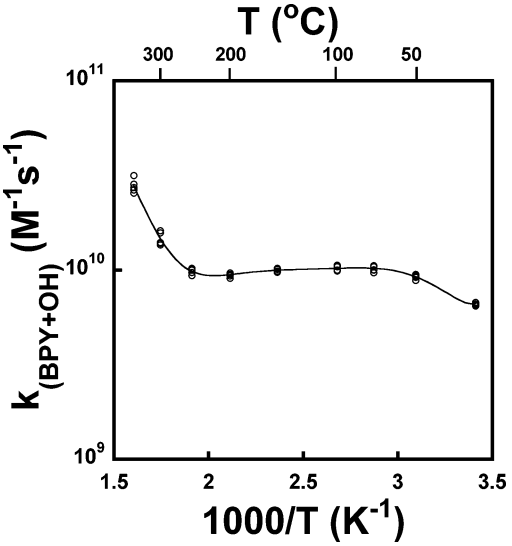

Figure 4. Arrhenius plot of the reaction between 4,4′-bpy and OH radical obtained by pulse radiolysis of 4,4′-bpy in N_2O-saturated aqueous solutions.

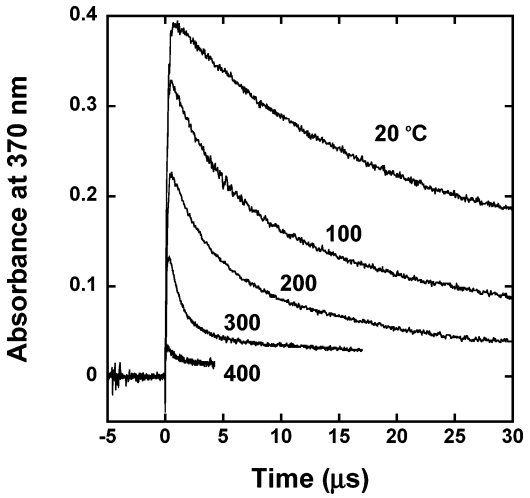

Figure 5. Time profiles at 370 nm of the decay of OH adducts to 4,4′-bpy obtained by pulse radiolysis of 0.5 mM 4,4′-bpy in N_2O-saturated solution at different temperatures. The pressure was 25 MPa for temperature range 20−300 °C and 30 MPa for 400 °C.

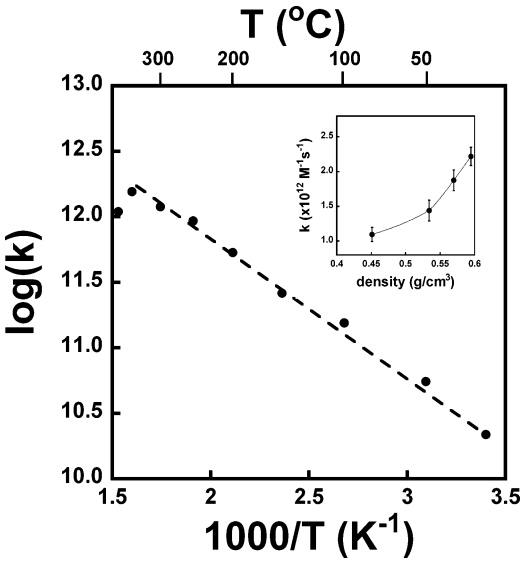

Figure 6. Arrhenius plot of the reaction between 4,4′-bpy and hydrated electron obtained by pulse radiolysis of 4,4′-bpy in Ar-saturated aqueous solutions. Inset: Log k as a function of density at 380 °C.

temperature to 350 °C at a constant pressure of 25 MPa. The rate constant is insensitive from room temperature to 250 °C but there is an increase above 250 °C.

Ashton et al.[32] have reported the nonlinear Arrhenius behavior of rate constants when they studied the reactions of •OH with aromatic compounds from room temperature to 200 °C. They proposed a mechanism that $[HOC_6H_5X]^\bullet$ radical is formed through an intermediate that can dissociate back to the reactants in competition with the forward step. The intermediate is a π-complex in which the electrophilic •OH interacts with the π-electrons of the aromatic ring as a precursor of the more stable σ-bonded $[HOC_6H_5X]^\bullet$. We suggest that this model is also applicable to 4,4′-bpy, and we propose the following mechanism:

$$^\bullet OH + 4,4'\text{-bpy} \rightarrow [4,4'\text{-bpyOH}]^\bullet_\pi \quad (6)$$

$$[4,4'\text{-bpyOH}]^\bullet_\pi \rightarrow {}^\bullet OH + 4,4'\text{-bpy} \quad (7)$$

$$[4,4'\text{-bpyOH}]^\bullet_\pi \rightarrow [4,4'\text{-bpyOH}]^\bullet_\sigma \quad (8)$$

Recently, Marin et al.[33] and Feng et al.[28] extended the study of the rates of reaction of nitrobenzene with •OH to supercritical water. An increase of rate constants at elevated temperature (above 300 °C) was reported. Both groups adopted the mechanism of Ashton et al.,[32] with more or less modification, succeeded in modeling the experimental data over the entire temperature range.

Figure 5 shows the decays of $[4,4'\text{-bpyOH}]^\bullet$ from room temperature to 400 °C. The decays mostly follow second-order law from 20 to 200 °C, but at 300 and 400 °C they do not obey either first- or second-order law. Therefore, in addition to reactions 6−8, the following reaction also should be included:

$$[4,4'\text{-bpyOH}]^\bullet + [4,4'\text{-bpyOH}]^\bullet \rightarrow \text{products} \quad (9)$$

And probably a hydrolysis reaction also takes place:

$$[4,4'\text{-bpyOH}]^\bullet \xrightarrow{-H_2O} \text{products} \quad (10)$$

From room temperature to 200 °C, reaction 9 is predominant and the decays show mostly second-order behavior. At higher temperatures, reactions 7 and 10 become more and more important, so the decay is much more complicated. According to Ashton et al.,[32] in the case of aromatic compounds, the rates and activation energies for the reactions similar to 7 were about 4.0×10^9 M^{-1} s^{-1} and 20 kJ/mol, respectively. So at 400 °C, the rate constant of reaction 7 could be 2 orders of magnitude higher, that is, 4.0×10^{11} M^{-1} s^{-1} (not taking into account the density effect).

Moreover, according to our previous work,[6] a general trend is that $\{G(e_{aq}^-) + G(OH) + G(H)\}$ increases with temperature at 25 MPa. This implies that the absorbance at λ_{max} would increase with temperature under the above-mentioned conditions. However, the experimental data show that the absorbance decreases quickly with increasing temperature (Figure 3). This can be well explained by the existence of reactions 7, 9, and 10.

3.3. Reaction of Hydrated Electron with 4,4′-Bpy. *3.3.1. Neutral Solution.* Figure 6 shows the Arrhenius plot of the reaction between hydrated electron and 4,4′-bpy. We measured the rate constants using deaerated solutions containing various concentrations of 4,4′-bpy in the presence of 10 mM *tert*-butyl alcohol. For the measurements, two HPLC pumps system were used. We prepared two bulk solutions, one containing only 10 mM *tert*-butyl alcohol and another containing 100 μM 4,4′-bpy and 10 mM *tert*-butyl alcohol. The concentration of the solutions passing through the high-temperature cell was adjusted by changing the flow rate of the two HPLC pumps. The pulse duration of the electron beam was 2 ns and the dose per pulse was about 8 Gy. The concentration ranges of 4,4′-bpy were different depending on temperature. For example, at room temperature, it was 40−80 μM, while at 350 °C, it was 25−40 μM. At each temperature, 3−4 concentrations were measured. At room temperature, the rate constant was determined to be 2.2×10^{10} M^{-1} s^{-1} at pH 7.2. This is in very good agreement with the reported values 2.5×10^{10} M^{-1} s^{-1} (at pH 8.3)[9] and 3.3×10^{10} M^{-1} s^{-1} (at pH 9.3).[8] The Arrhenius plot shows a linear relationship between log k and $1/T$ for temperatures $\leq$ 350 °C. An activation energy of 19.6 kJ/mol was obtained within this temperature range. This value is very close to that of methyl viologen.[6] The inset of Figure 6 shows density dependence of rate constants at 380 °C. Similar behavior has been observed previously by Cline et al.[34] for the reactions of solvated electrons with SF_6 and O_2, etc.

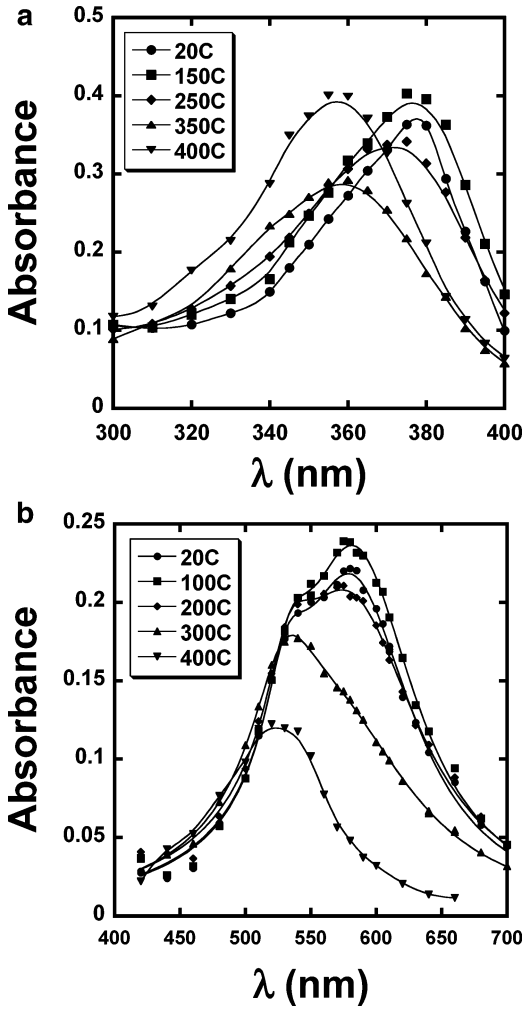

Figure 7. Pulse radiolysis of 0.5 mM 4,4′-bpy solutions in the presence of 0.2 M *tert*-butyl alcohol at pH 7.4, observed at 300 ns. The pressure was 25 MPa for temperature range 25−350 °C and 30 MPa for 400 °C. (a) UV region, dose = 43 Gy; (b) visible region, dose = 49 Gy.

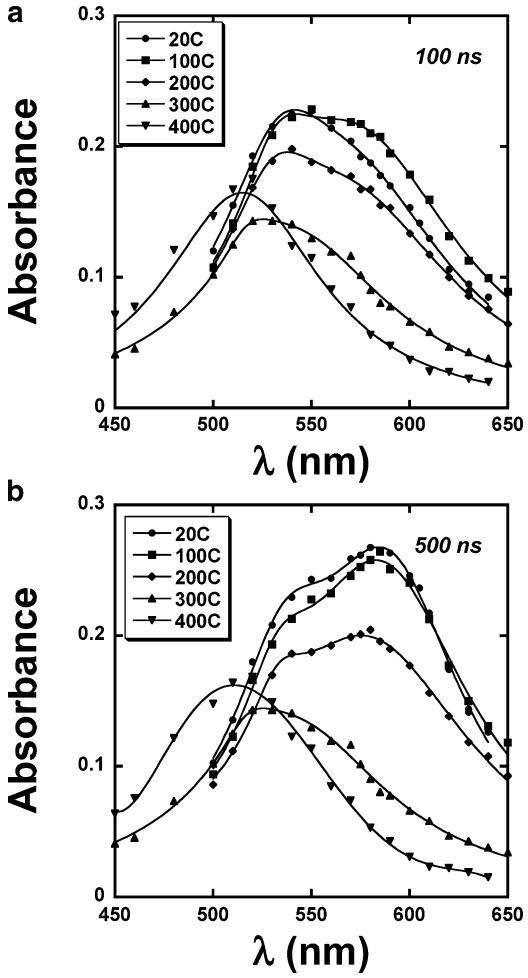

Figure 8. Temperature-dependent transient absorption spectra of electron adducts to 4,4′-bpy obtained by pulse radiolysis of 5 mM 4,4′-bpy/0.2 M *tert*-butyl alcohol in Ar-saturated aqueous solutions recorded at (a) 100 ns and (b) 500 ns.

Figure 7 shows the absorption spectra of the electron adduct to 4,4′-bpy, which were obtained by pulse radiolysis of an aqueous solution containing 0.5 mM 4,4′-bpy and 0.2 M *tert*-butyl alcohol at pH 7.4. Figure 7a shows the temperature-dependent spectra in the UV region. At room temperature, a very sharp absorption band is located at λ_{max} = 375 nm. With increasing temperature, the component at λ_{max} = 375 nm becomes smaller and smaller, the absorbance at 360 nm increases, and at 400 °C/30 MPa, λ_{max} = 360 nm. Figure 7b shows the temperature-dependent spectra in the visible region. At room temperature, a broad absorption band is located at λ_{max} = 580 nm with a shoulder at about 530 nm. With increasing temperature, the component at λ_{max} = 580 nm becomes smaller, the absorbance at 530 nm increases, and at 400 °C/30 MPa, the transient species at 530 nm becomes predominant. From the similarity of kinetics at 375 and 580 nm as well as the ratio of A_{375nm}/A_{360nm} and A_{580nm}/A_{530nm}, the entity at 375 and 580 nm is considered to be the same entity, which has been attributed to 4,4′-bpy$H_2^{+\bullet}$.[9] The entity at 360 and 530 nm is also the same component but it is not 4,4′-bpy$H_2^{+\bullet}$. From the similarity of spectra and Figure 2, we attributed it to 4,4′-bpyH$^\bullet$. The following facts also strongly support our attribution.

Figure 8 was obtained by pulse radiolysis of an aqueous solution containing 5 mM 4,4′-bpy and 0.2 M *tert*-butyl alcohol at pH 7.4. Under these conditions, at room temperature the scavenging rate constant of 4,4′-bpy to hydrated electron is 1.1×10^8 s^{-1}. This means the reaction completes within 10 ns. The spectra in Figure 8a were recorded at 100 ns after the electron pulse, while those in Figure 8b were recorded at 500 ns. A comparison of the these figures reveals that, at temperatures < 300 °C, a component at about 530 nm appears first at shorter time and evolves to form a component at about 580 nm, but this evolution became less important with increasing temperature. Above 350 °C, almost no evolution of the spectra was observed. Therefore, we suppose the formation of electron adduct of 4,4′-bpy follows the mechanism

$$e_{aq}^- + \text{4,4′-bpy} \xrightarrow{H^+ \text{ or } H_2O} \text{4,4′-bpyH}^\bullet \xleftrightarrow{H^+} \text{4,4′-bpyH}_2^{+\bullet} \quad (11)$$

At lower temperatures, the reaction of e_{aq}^- with 4,4′-bpy produced 4,4′-bpyH$^\bullet$, which may quickly associate a proton to form 4,4′-bpy$H_2^{+\bullet}$ and they reach equilibrium. With increasing temperature, the equilibrium reaction 4 is favorable for the right side; thus 4,4′-bpyH$^\bullet$ becomes predominant. In supercritical water, the ion product of water is so small (e.g., at 400 °C/25 MPa, pK_w = 19.43) that 4,4′-bpyH$^\bullet$ could not associate with H^+. Consequently, only 4,4′-bpyH$^\bullet$ is observed.

Therefore, from the above results, we know that at temperatures < 350 °C, there exist in fact two transient species, 4,4′-bpyH$^\bullet$ and 4,4′-bpy$H_2^{+\bullet}$. Unlike methyl viologen, it is rather

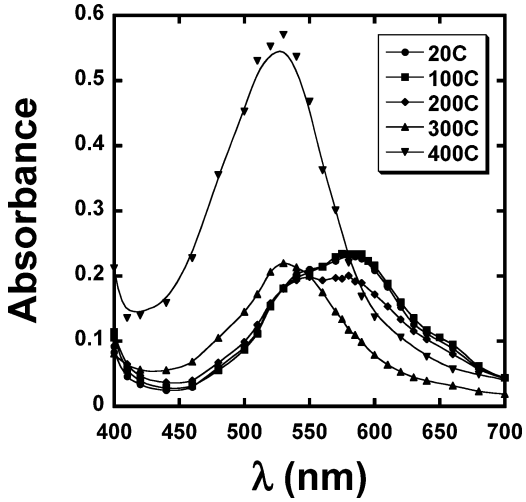

Figure 9. Pulse radiolysis of 0.5 mM 4,4′-bpy solutions in the presence of 10 mM NaCOOH at pH 7.4. The pressure was 25 MPa for temperature range 25−350 °C and 30 MPa for 400 °C. Dose: 60 Gy.

difficult to use 4,4′-bpy as a scavenger to estimate $G(e_{aq}^-)$ in this temperature range. However, in supercritical water conditions, there is only a single component, 4,4′-bpyH•, so the estimation of $G(e_{aq}^-)$ would be possible.

The absorption spectra in Figure 9 were obtained by pulse radiolysis of an aqueous solution containing 0.5 mM 4,4′-bpy and 10 mM NaCOOH at pH 7.4. It shows almost the same spectrum as in the presence of *tert*-butyl alcohol at room temperature (Figure 7). However, here we show only the spectra in the visible region. Again, with increasing temperature, the absorbance at 580 nm becomes smaller and that at 530 nm becomes predominant at 400 °C/30 MPa (in fact, from 350 °C/25 MPa). But different from the case in the presence of *tert*-butyl alcohol, at 400 °C/30 MPa, it shows a much higher absorbance.

In addition, a similar study with ethanol as a scavenger from room temperature to 350 °C shows the same spectral property as *tert*-butyl alcohol but not as NaCOOH.

To elucidate the above spectral data, we need to look at the kinetic behavior of the formation of the transient from 4,4′-bpy. Figure 10a shows the time profiles at 530 nm at different temperatures obtained by pulse radiolysis of a deaerated solution of 0.5 mM 4,4′-bpy in the presence of 0.2 M *tert*-butyl alcohol, while Figure 10b is in the presence of 10 mM NaCOOH. From both figures, we can clearly see the decay of hydrated electron and the formation of 4,4′-bpyH• and also the evolution to 4,4′-$bpyH_2^{+}$• at room temperature. With increasing temperature, the reaction between hydrated electron and 4,4′-bpy becomes faster. In the case of *tert*-butyl alcohol, the absorbance decreases with increasing temperature: at 400 °C/30 MPa we observed a fairly stable product. In the presence of NaCOOH, at temperatures < 200 °C, the temperature-dependent time profiles are almost the same as for *tert*-butyl alcohol. However, at 300 °C/25 MPa, we observed a slow formation process. At 350 °C/25 MPa, the formation of a transient can be completely observed within a 2 μs time window. At 400 °C/30 MPa, the formation finishes within 400 ns and reaches a plateau. The absorbance at 400 °C is much higher than that in the presence of *tert*-butyl alcohol.

Figure 11 shows the time profiles at 350 °C/25 MPa in the presence of *tert*-butyl alcohol, ethanol, and NaCOOH. Surprisingly, unlike the scavenging system of methyl viologen in our previous study,[6] ethanol acts like *tert*-butyl alcohol but not like NaCOOH. The kinetic signal of NaCOOH obviously consists of two parts. One is a very fast formation process, which has

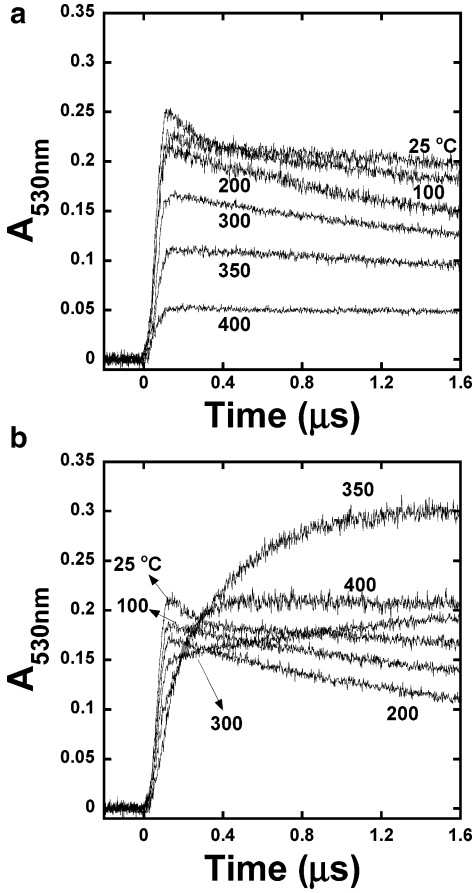

Figure 10. Temperature-dependent time profiles at 530 nm for electron adducts of 4,4′-bpy obtained by pulse radiolysis of deaerated aqueous solutions of 0.5 mM 4,4′-bpy in the presence of (a) 0.2 M *tert*-butyl alcohol and (b) 10 mM NaCOOH at pH 7.4.

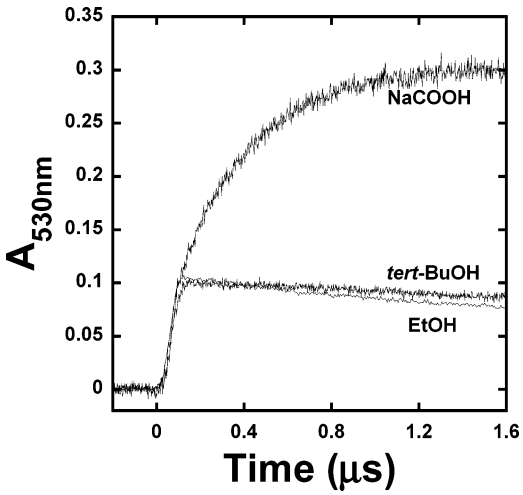

Figure 11. Time profiles at 530 nm obtained by pulse radiolysis of deaerated aqueous solutions of 0.5 mM 4,4′-bpy in the presence of 10 mM NaCOOH, 0.2 M *tert*-butyl alcohol, or 0.2 M ethanol at pH 7.4, at $T = 350$ °C.

the same magnitude (absorbance) as the alcohols; another is a formation process with $t_{1/2} \approx 100$ ns. All the facts above allow us to propose the mechanism below: for *tert*-butyl alcohol and ethanol, their role is to scavenge OH radical and H atom, so we observed 4,4′-bpyH• and 4,4′-$bpyH_2^{+}$• at temperatures < 300 °C and observed only 4,4′-bpyH• at temperatures > 350 °C. For NaCOOH, at temperatures < 300 °C, it behaves like the alcohols, but at temperatures > 300 °C, OH radical and H

atom also have contributions to the formation of 4,4′-bpyH•.

$$OH + HCO_2^- \rightarrow CO_2^{-\bullet} + H_2O \qquad k_{12} = 3.2 \times 10^9\ M^{-1}\ s^{-1}\ (\text{ref } 35) \quad (12)$$

$$H + HCO_2^- \rightarrow CO_2^{-\bullet} + H_2 \qquad k_{13} = 2.1 \times 10^8\ M^{-1}\ s^{-1}\ (\text{ref } 36) \quad (13)$$

$$4,4'\text{-bpy} + CO_2^{-\bullet} \rightarrow 4,4'\text{-bpy}^{-\bullet} + CO_2 \quad (14)$$

Then the radical anion 4,4′-bpy$^{-\bullet}$ undergoes rapid protonation (with free H^+ or H_2O) on nitrogen to form 4,4′-bpyH•.

No literature data of a rate constant is available for reaction 14. However, in a study of 2,2′-bipyridyl, Mulazzani et al.[11] pointed out that the rate constant of the reaction of $CO_2^{-\bullet}$ with 2,2′-bipyridyl is $<1 \times 10^6\ M^{-1}\ s^{-1}$ at room temperature. Evidently, from our experimental results, reaction 14 also proceeds with a rather low rate constant. The reaction is accelerated by increasing temperature, so that at temperatures > 300 °C we observed a formation process. A rough estimation of the formation at 350 °C gives us a rate constant of $6 \times 10^9\ M^{-1}\ s^{-1}$. If the rate constant at room temperature is taken as $1 \times 10^6\ M^{-1}\ s^{-1}$, then we can roughly derive an activation energy >44 kJ/mol from the rate constants of these two temperatures. In addition, in Figure 11, the ratio of the maximum absorbance $A_{\text{formate}}/A_{\text{alcohol}}$ is around 3; this agrees very well with our previous result, where the ratio $\{G(e_{aq}^-) + G(OH) + G(H)\}/G(e_{aq}^-)$ at 350 °C/25 MPa was $10.05/3.4 \approx 3$.[6]

Although e_{aq}^- reduces 4,4′-bpy at a diffusion-controlled rate, $CO_2^{-\bullet}$ and CH_3•CHOH show no reactivity in pulse radiolysis at room temperature. CH_3•CHOH is unable to reduce 4,4′-bpy even up to 350 °C, while $CO_2^{-\bullet}$ can react with it but with a rather high activation energy. This implies that the redox potential of 4,4′-bpy would lie between those of $CO_2^{-\bullet}$ and CH_3•CHOH, that is, between −1.90[37] and −1.1 V versus NHE.[38] This estimation is reasonable as compared with the literature data on that of 2,2′-bpy ($E_{1/2} = -1.33$ V versus SCE in 0.1 N KC1).[39]

Therefore, 4,4′-bpy/NaCOOH scavenging system is not applicable for the estimation of $\{G(e_{aq}^-) + G(OH) + G(H)\}$ when the temperature is lower than 350 °C. But it would be suitable for supercritical water. It is also worth noting that even at 400 °C/30 MPa the apparent absorbance (without correction for density) is still fairly high, for example, about 0.2 in Figure 9. This is an advantage for obtaining accurate data for low-density supercritical water, especially temperatures over 400 °C.

However, even if we do not know the temperature-dependent absorption coefficients at different temperatures, we can combine the two scavenging systems, that is, 4,4′-bpy/*tert*-butyl alcohol and 4,4′-bpy/NaCOOH, to obtain the information about the ratio of $\{G(e_{aq}^-) + G(OH) + G(H)\}/G(e_{aq}^-)$, where we need only to measure the absorbencies at λ_{max} for both systems (and the dose if they are measured under different beam conditions). As an example, although it is not very precise, from Figures 7b and 9 we can obtain a value of $\{G(e_{aq}^-) + G(OH) + G(H)\}/G(e_{aq}^-) \approx 3.8$. This is comparable to the value obtained in our previous study, which was 3.5.[6]

3.3.2. Alkaline Solution. Figure 12 was obtained by pulse radiolysis of a deaerated solution of 0.5 mM 4,4′-bpy in the presence of 0.2 M *tert*-butyl alcohol. The pH of the solution was adjusted to 11.5 by addition of NaOH. The pressure was 25 MPa for all temperatures. There is a very slight blue shift

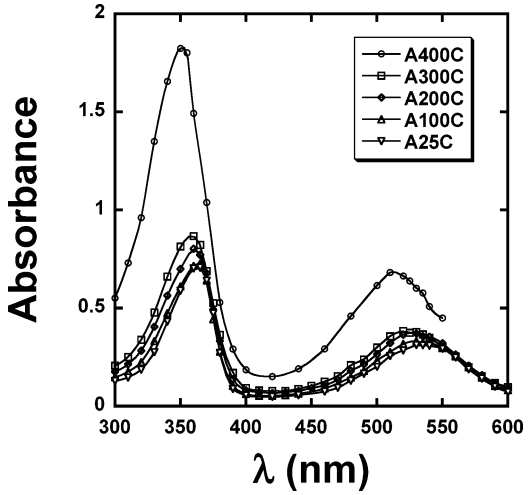

Figure 12. Pulse radiolysis at various temperatures of 0.5 mM 4,4′-bpy/0.2 M *tert*-butyl alcohol in deaerated aqueous solution at pH 11.5. The pressure was 25 MPa for all temperatures and the dose per pulse was 78.5 Gy.

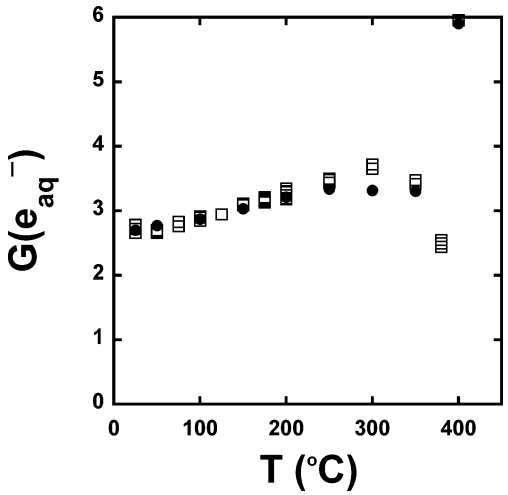

Figure 13. Comparison of temperature-dependent $G(e_{aq}^-)$ at 25 MPa obtained by use of different scavengers: (●) 4,4′-bpy, this work; (□) methyl viologen, ref 6.

from 535 to 525 nm within the temperature range 25−300 °C. But at 400 °C, the blue shift is much more notable, about 15 nm shift, as compared to 300 °C. The spectra in Figure 12 have been corrected for density. The absorbencies at λ_{max} gradually increase with temperature from 25 to 300 °C while the absorbance sharply increases at 400 °C.

On the basis of Figure 12, with an assumption that the absorption coefficient at peak position is temperature-independent and taking $G(e_{aq}^-) = 2.7$ for room temperature, we can obtain $G(e_{aq}^-)$ versus temperature plot, as shown in Figure 13 (●). $G(e_{aq}^-)$ increases with temperature up to about 300 °C and there is a sharp increase at 400 °C. In this figure, we include also the experimental data obtained in our recent study with methyl viologen as a scavenger.[6] Obviously, the results of the two scavenging systems are in fairly good agreement within the experimental error.

However, although the alkaline solution of 4,4′-bpy allows us to estimate $G(e_{aq}^-)$ at elevated temperatures, it is rather difficult to apply to temperatures higher than 400 °C. In fact, even at 400 °C, the sapphire windows corroded severely by the alkaline solution and they were easily broken during the experiments.

4. Conclusion

4,4′-Bpy is one of the few organic scavengers that is applicable for supercritical water without the problem of pyrolysis. For neutral pH solutions in the presence of *tert*-butyl alcohol, ethanol, or formate at room temperature, the doubly protonated electron adduct is the predominant transient species, while in supercritical water, only monoprotonated electron adduct could be observed. For 4,4′-bpy/formate scavenging system, the activation energy of the reaction between 4,4′-bpy and $CO_2^{-\bullet}$ is so high that it is difficult to observe at room temperature by pulse radiolysis, but at $T > 300$ °C, this reaction is observable. Consequently, if 4,4′-bpy/*tert*-butyl alcohol is used to measure $G(e_{aq}^-)$, 4,4′-bpy/formate can be applied to estimate $\{G(e_{aq}^-) + G(OH) + G(H)\}$ in supercritical water. Even if we do not know the temperature-dependent absorption coefficient of 4,4′-bpyH$^\bullet$, we may obtain the ratio of $\{G(e_{aq}^-) + G(OH) + G(H)\}/G(e_{aq}^-)$ at a given temperature/pressure condition. Both of the above scavenging systems are expected to be applicable to temperatures > 400 °C, and the studies have been ongoing.

Acknowledgment. This work was supported by the Ministry of Education, Culture, Sports, Science and Technology (MEXT), Japanese Government, as a "Fundamental R&D program on water chemistry of supercritical pressure water under radiation field".

References and Notes

(1) Savage, P. E.; et al. *AIChE J*. **1995**, *41*, 1723.
(2) Savage, P. E. *Chem. Rev.* **1999**, *99*, 603.
(3) Schmieder, H.; Abeln, J. *Chem. Eng. Technol.* **1999**, *22*, 903.
(4) Akiya, N.; Savage, P. E. *Chem. Rev.* **2002**, *102*, 2725.
(5) Oka, Y. *Proceedings 1998 Frederic Joliot Summer School in Reactor Physics*; August 1998, Cadarache, France; CEA: Cadarache, 1998; pp 240−259 and references cited therein.
(6) Lin, M.; Katsumura, Y.; Muroya, Y.; He, H.; Wu, G.; Han, Z.; Miyazaki, T.; Kudo, H. *J. Phys. Chem. A* **2004**, *108*, 8287.
(7) Yamaji, A.; Oka, Y.; Koshizuka, S. *Proceedings of Global2003 Conference*, New Orleans, LA; American Nuclear Society, Inc.: La Grange Park, IL, 2003.
(8) Simić, M.; Ebert, M. *Int. J. Radiat. Phys. Chem.* **1971**, *3*, 259.
(9) Solar, S. *J. Phys. Chem.* **1979**, *88*, 5624.
(10) Please refer to IAPWS Web site: http://www.iapws.org.
(11) Mulazzani, Q. G.; Emmi, S.; Fuochi, P. G.; Venturl, M.; Hoffman, M. Z.; Simić, M. G. *J. Phys. Chem.* **1979**, *83*, 1582.
(12) Venturi, M.; Mulazzani, Q. G.; Hoffman, M. Z. *Radiat. Phys. Chem.* **1984**, *23*, 229.
(13) (a) Poizat, O.; Buntinx, G.; Ventura, M.; Lautié, M. F. *J. Phys. Chem.* **1991**, 95, 1245. (b) Buntinx, G.; Valat, P.; Wintgens, V.; Poizat, O. *J. Phys. Chem*. **1991**, *95*, 9347. (c) Poizat, O.; Buntinx, G.; Valat, P.; Wintgens, V.; Bridoux, M. *J. Phys. Chem.* **1993**, *97*, 5905. (d) Buntinx, G.; Naskrecki, R.; Poizat, O. *J. Phys. Chem.* **1996**, *100*, 19380. (e) Boilet, L.; Burdzinski, G.; Buntinx, G.; Lefumeux, C.; Poizat, O. *J. Phys. Chem. A* **2001**, *105*, 10271.
(14) (a) Paraquat Fact Sheet. *Pesticides News*, Pesticides Action Network UK: 1996; No. 32. http://www.gn.apc.org/pesticidestrust. (b) The Extension Toxicology Network (EXTOXNET), Oregon State University; http://ace.ace.orst.edu/info/extoxnet.
(15) Web page of Pesticides Action Network North America: http://www.panna.org/resources/panups/panup_20031203.dv.html
(16) Florêncio, M. H.; Pires, E.; Castro, A. L.; Nunes, M. R.; Borges, C.; Costa, F. M. *Chemosphere* **2004**, *55*, 345.
(17) Hamadi, N. K.; Swaminathan, S.; Chen, X. D. *J. Hazard. Mater*. **2004**, *B112*, 133.
(18) Wu, G.; Katsumura, Y.; Muroya, Y.; Li, X.; Terada, Y. *Chem. Phys. Lett*. **2000**, *325*, 531.
(19) Mostafavi, M.; Lin, M.; Wu, G.; Katsumura, Y.; Muroya, Y. *J. Phys. Chem. A* **2002**, *106*, 3123.
(20) Buxton, G. V.; Stuart, C. R. *J. Chem. Soc., Faraday Trans.* **1995**, *91*, 279.
(21) Linnell, R. H.; Kacymarczyk, A. *J. Phys. Chem.* **1961**, *65*, 1196.
(22) Schulman, S. G.; Tidwell, P. T.; Cetorelli, J. J.; Winefordner, J. D. *J. Am. Chem. Soc.* **1971**, *93*, 3179.
(23) Kihara, H.; Gondo, Y. *J. Raman Spectrosc*. **1985**, *17*, 263.
(24) Hiratsuka, H.; Sekiguchi, K.; Hatano, Y.; Tanizaki, Y.; Mori, Y. *Can. J. Chem*. **1987**, *65*, 1184.
(25) Shida, T. *Electronic Absorption Spectra of Radical Ions*; Elsevier: Amsterdam, 1988; p 198.
(26) Fessenden, R. W.; Neta, P. *Chem. Phys. Lett*. **1973**, *18*, 14.
(27) Janata, E.; Schuler, R. H. *J. Phys. Chem*. **1982**, *86*, 2078.
(28) Feng, J. B.; Aki, S. N. V. K.; Chateauneuf, J. E.; Brennecke, J. F. *J. Am. Chem. Soc*. **2002**, *124*, 6304.
(29) Reichardt, C. *Chem. Rev*. **1994**, *94*, 2319.
(30) Bennett, G. E.; Johnston, K. P. *J. Phys. Chem*. **1994**, *98*, 441.
(31) Nielsen, S. O.; Michael, B. D.; Hart, E. J. *J. Phys. Chem*. **1976**, *80*, 2482.
(32) Ashton, L.; Buxton, G. V.; Stuart, C. R. *J. Chem. Soc., Faraday Trans*. **1995**, *91*, 1631.
(33) Marin, T. W.; Cline, J. A.; Takahashi, K.; Jonah, C. D.; Bartels, D. M. *J. Phys. Chem. A* **2002**, *106*, 12270.
(34) Cline, J. A.; Takahashi, K.; Marin, T. W.; Jonah, C. D.; Bartels, D. M. *J. Phys. Chem. A* **2002**, *106*, 12260.
(35) Mulazzani, Q. G.; D'Angelantonio, M.; Venturi, M.; Hoffman, M. Z.; Rodgers, M. A. J. *J. Phys. Chem.* **1986**, *90*, 5347.
(36) Farrington, J. A.; Ebert, M.; Land, E. J.; Fletcher, K. *Biochim. Biophys. Acta* **1973**, *314*, 372.
(37) Schwarz, H. A.; Creutz, C.; Sutin, N. *Inorg. Chem*. **1985**, *24*, 433.
(38) Asmus, K. D.; Möckel, H.; Henglein, A. *J. Phys. Chem*. **1973**, *77*, 1218.
(39) Gurtier, O.; Dietz, K. P.; Thomas, P. *Z. Anorg. Allg. Chem.* **1973**, *396*, 217.